THE JOURNAL OF PHYSICAL CHEMISTRY A

Article

Cite This: J. Phys. Chem. A 2019, 123, 103−110

pubs.acs.org/JPCA

Experimental and Theoretical Investigation of the Pyrolysis of Furfural

Published as part of The Journal of Physical Chemistry virtual special issue "William M. Jackson Festschrift".

Yamin Li,[†] Qinghui Meng,[†] Jinglan Wang,[‡] Yan Zhang,[†] Chuangchuang Cao,[†] Zhanjun Cheng,*[,‡] Jiuzhong Yang,[†] Fuyi Liu,[†] Lidong Zhang,*[,†] and Yang Pan*[,†]

[†]National Synchrotron Radiation Laboratory, University of Science and Technology of China, Hefei, Anhui 230029, People's Republic of China

[‡]School of Environmental Science and Engineering, Tianjin University, Tianjin 300072, People's Republic of China

Supporting Information

ABSTRACT: The thermal decomposition of furfural is investigated in a flow tube reactor at 30 Torr by synchrotron vacuum ultraviolet photoionization mass spectrometry (SVUV-PIMS) at temperatures from 1023 to 1273 K. Over 20 kinds of pyrolysis products, including short-lived radicals, stable oxygen-containing compounds, and hydrocarbons, are identified from the scanning photoionization efficiency (PIE) spectra. Vinylketene (CH_2═CH−CH═C═O), which has been shown to be an important primary product, is also directly observed. The possible steps of hydrogen atom addition and hydrogen atom abstraction in the thermal decomposition of furfural are studied by theoretical calculations at the CBS-QB3 level. In addition to unimolecular decomposition, hydrogen atom addition followed by ring opening can lead to the production of vinylketene.

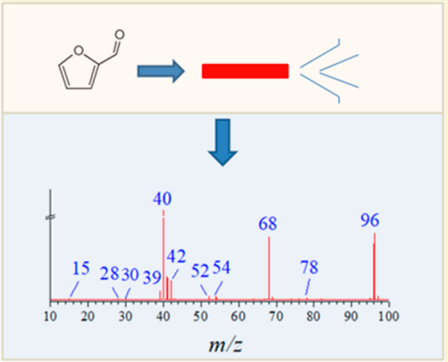

INTRODUCTION

Biomass has attracted widespread attention in recent years because it is not only an abundant raw material but also the only renewable source of carbon found in nature. In particular, the bio-oil obtained through the thermal decomposition conversion of biomass is regarded as a potential biochemical alternative to liquid transport fuel.[1−3] Furan and its derivatives are emerging but promising biofuels.[4−6] As the common species in bio-oil, it is of great interest to study the mechanisms of the pyrolysis of furan compounds because pyrolysis conversion is an indispensable stage of combustion.[7,8] The majority of pioneering studies have mainly focused on the pyrolytic mechanism of furan and methylfuran.[9−14] In previous studies, furan was reported to initially decompose to CO + propyne, acetylene + ketene, and propargyl radical + H + CO through a unimolecular reaction.[9,10,13] Cheng et al. reported that the contributions of the hydrogen atom addition and hydrogen atom abstraction reactions by hydrogen atom attack to the consumption of furan are both less than 1%,[9] which is quite different from the consumption of 2-methylfuran. Somers et al. and Cheng et al. observed that the thermal hydrogen atom addition and hydrogen atom abstraction reactions mainly contributed to the consumption of 2-methylfuran.[12,14] The hydrogen atom attack reaction was beneficial for the formation of furan + methyl radical, vinylketene + methyl radical, and 1-butene-1-yl radical + CO.[12] In addition, hydrogen atom attack reactions are prominent in the pyrolysis of benzaldehyde, the simplest aldehyde derivative of benzene.[15] Hence, the reactions of hydrogen atom attack on furfural should play an important role in the process of furfural pyrolysis, owing to furfural being the simplest aldehyde derivative of furan.

Furfural (2-furaldehyde) is an important intermediate in the thermal conversion process of biomass.[1,16,17] Moreover, furfural also acts as a base chemical for the production of fuels and fine chemicals. In the past several decades, the thermal decomposition mechanisms of furfural have been studied by four groups. Hurd et al. first reported that the pyrolysis of furfural produced furan and CO in 1932.[18] Grela et al. studied the pyrolysis of furfural in a flow reactor at a very low pressure by using modulated beam mass spectrometry above 1090 K.[19] They proposed that vinylketene (CH_2═CH−CH═C═O) and CO were the initial products formed through ring opening followed by hydrogen atom transfer. Vasiliou et al. investigated the thermal decomposition of furfural in a microtubular flow reactor in the pressure range of 75−150 Torr and the temperature range of 1200−1800 K.[15] The products were identified by photoionization mass spectrometry and infrared spectrometry. They proposed that the decomposition process was initialized by furfural pyrolysis to furan and CO through a unimolecular decomposition

Received: June 30, 2018
Revised: November 16, 2018
Published: December 3, 2018

DOI: 10.1021/acs.jpca.8b06261
J. Phys. Chem. A 2019, 123, 103−110

reaction, followed by furan pyrolysis into acetylene, ketene, propargyl radical, propyne, and other products.[15] Recently, Vermeire et al. studied the pyrolysis of furfural in a jet-stirred reactor at atmospheric pressure and 900−1000 K.[20] The unimolecular nonradical decomposition channel through α-pyrone was confirmed as the main channel. The elimination of CO and the formation of CO_2 were also discussed. In these above-mentioned studies, vinylketene was proposed and argued to be the vitally initial product. However, no direct experimental evidence has been afforded. The high energy resolution and broad energy tunability of synchrotron VUV light are beneficial for distinguishing most isomers and facilitate the detection of radicals and unambiguous intermediates. In addition, the pyrolytic mechanism of furfural has only been understood on the basis of the unimolecular decomposition reaction, while the hydrogen atom addition and hydrogen atom abstraction reactions are poorly understood. Therefore, a comprehensive mechanistic picture of furfural pyrolysis is still to be determined.

This paper reports the thermal decomposition of furfural in a flow tube reactor at 30 Torr and temperatures of 1023−1273 K. Pyrolysis products were detected by synchrotron vacuum ultraviolet photoionization mass spectrometry (SVUV-PIMS) and were further characterized from scanning photoionization efficiency (PIE) spectra. To gain greater insight into the pyrolysis processes of furfural, theoretical calculations were performed to depict the hydrogen atom addition and hydrogen atom abstraction reactions, which can provide guidance for the rational design and further potential application of the thermal conversion system of furfural.

EXPERIMENTAL AND THEORETICAL METHODS

Experimental Procedure. The pyrolysis of furfural was performed at the National Synchrotron Radiation Laboratory (NSRL) in Hefei, China. Details of the beamline and the pyrolysis apparatus have been reported elsewhere;[21−23] therefore, only a brief description is given here. Synchrotron radiation from an undulator beamline (BL03U) was monochromatized with a 200 lines/mm laminar grating (Horiba Jobin Yvon, France), which covered the photon energy from 7.5 to 22 eV with an energy resolving power of 3000 ($E/\Delta E$ @ 10 eV). A gas filter filled with noble gas was used to suppress the high-order harmonic radiation. The average photon flux could reach a magnitude of 10^{13} photons/s. A silicon photodiode (SXUV-100, International Radiation Detectors, Inc., U.S.A.) was used to monitor the photon flux to normalize the ion signals.

The thermal decomposition apparatus was mainly composed of a pyrolysis chamber with an electrically heated flow tube, a differentially pumped molecular beam sampling system, and a photoionization chamber equipped with a homemade reflectron time-of-flight mass spectrometer (RTOF).[24] Figure 1a shows a schematic diagram and temperature profiles of the flow tube pyrolysis apparatus. The flow tube (i.d. 7 mm, length 224 mm) was made of α-Al_2O_3 to reduce the wall catalytic effect.[40,41] An S-type thermocouple was used to measure the temperature along the centerline of the flow tube. The pressure of the pyrolysis chamber was maintained at 30 Torr. Furfural (99%, Aladdin Chemical Reagent Co. Ltd., China) evaporated with a homemade vaporizer and diluted with Ar (99.999%) was flowed into the flow tube with a total flow rate of 1.0 standard liter per minute (SLM) at 273.15 K. The mole fraction of furfural was 0.01. The pyrolysis products were sampled 5 mm downstream from the tube outlet by a quartz nozzle. The formed molecular beam passed through a nickel skimmer into the photoionization chamber and was ionized by crossed synchrotron VUV light. The generated ions were mass-analyzed by the RTOF. The output ion signals were amplified by a preamplifier (VT120C, ORTEC, U.S.A.) and recorded with a 1 GHz multiscaler (P7888, FAST Comtec, Germany).[25−27]

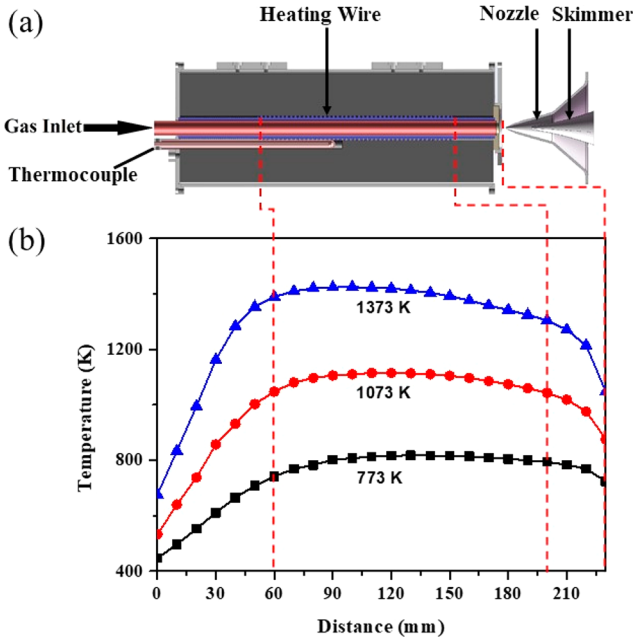

Figure 1. (a) Schematic diagram of the flow reactor pyrolysis apparatus and (b) three measured centerline temperature profiles along the tube at 773, 1073, and 1373 K.

The PIE spectra were obtained by scanning the photon energy with a step size of 0.05 eV and accumulation time of 200 s for each mass spectrum. To eliminate the influence of photon flux variations on the photon energy, all of the ion signals were normalized by the monitored photon flux.

Theoretical Calculations. All of the quantum chemistry calculations were conducted using the Gaussian 09 program.[28] The geometry optimization of the reactants, transition states, intermediates, and products was primarily performed using the M06-2X density functional method with the cc-pVTZ basis set, followed by the high-precision calculation method CBS-QB3. Transition states were verified as those possessing a reasonable geometry with only one imaginary frequency, whose atomic displacement appeared to approximate the desired reaction coordinate through visual inspections.

RESULTS AND DISCUSSION

Identification of Furfural Pyrolysis Products. The photoionization mass spectra of furfural pyrolysis products, which were recorded at a fixed energy of 11 eV and pyrolysis temperatures of 1023−1273K, are displayed in Figure 2. At 1023 K, some early pyrolysis product peaks at m/z = 68, 42, 40, 39, 30, and 28 were clearly observed. With the increase of the temperature, some new mass peaks at m/z of 78, 54, 52, and 15 were formed. The intensity of the m/z = 96 peak declined considerably, while the other peaks showed different tendencies.

DOI: 10.1021/acs.jpca.8b06261
J. Phys. Chem. A 2019, 123, 103−110

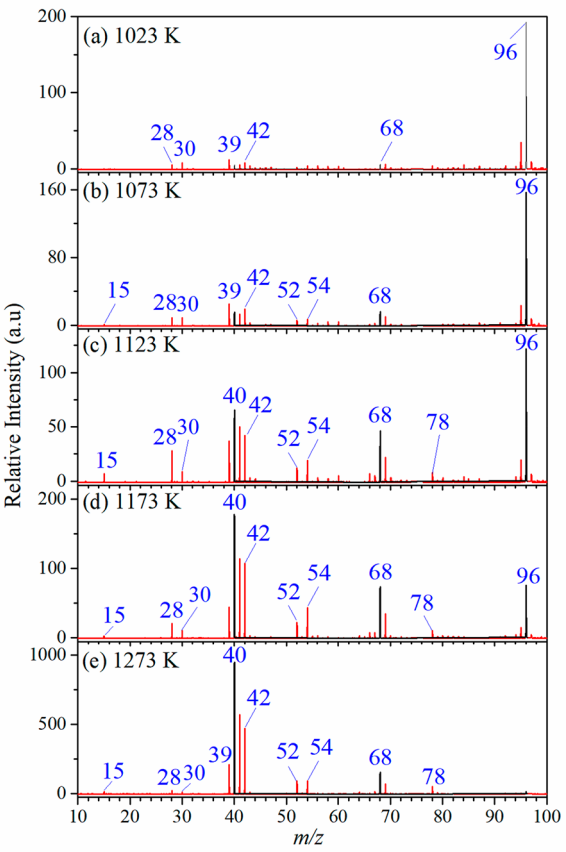

Figure 2. Mass spectra of furfural pyrolysis at a photon energy of 11 eV with various thermal decomposition temperatures under 30 Torr: (a) 1023, (b) 1073, (c) 1123, (d) 1173, and (e) 1273 K. The intensities of the m/z = 40, 68, and 96 peaks are reduced by factors of 20, 10, and 100, respectively.

To further identify the pyrolysis products and discriminate the possible isomers, the PIE curve of each mass peak was measured by plotting the ion intensity versus the corresponding photon energy. Figure 3 shows the PIE spectra of some representative species resulting from the thermal decomposition of furfural at a temperature of 1273 K.

As shown in Figure 3a,b, clear onsets at 9.82 and 8.65 eV were observed for the m/z = 15 and 39 ions, which indicated the presences of unstable methyl radical (CH_3) and propargyl radical ($CH_2{-}C{\equiv}CH$), reported in the pyrolysis of furan.[9,10,29,30] Both of the radicals were mainly formed from propyne ($CH_3{-}C{\equiv}CH$).[9] From Figure 3c,e, ethylene and ketene were identified to exist from the onsets at 10.53 eV of m/z = 28 and 9.63 eV of m/z = 42.[31,32] Both of these species were the decomposition products of furan.[9,10] In the case of Figure 3d, two thresholds near 9.72 and 10.33 eV were observed, which corresponded to the ionization energies (IEs) of allene and propyne.[32] In previous work, only propyne was determined for this mass peak.[15,20] Here, an equilibrium with a [propyne]/[allene] ratio of 7 could be calculated by simulating the experimental PIE curve with scaled absolute photoionization cross sections (PICSs) of propyne and allene. The relative photoionization cross section simulated for m/z = 42 is shown in Figure 3e. The simulated curve, which represented the best-fit isomeric composition of 60% ketene and 40% propene, was in good agreement with the experimental data.[32] Figure 3f exhibited only one onset at 9.07 eV of m/z = 54 ions, which was ascribed to the IE of 1,3-butadiene.[32] By simulating the PIE spectrum with known PICSs, 1-butyne and 2-butyne were also distinguished.[32] In addition, 2-propynal (IE = 10.62 eV),[33] a short-lived product in furfural pyrolysis by theoretical calculation,[20] was also found to exist by simulation. The most interesting result was observed in Figure 3g, where vinylketene (IE = 8.42 eV) could be unambiguously confirmed through a clear onset on the PIE curve, in addition to the formation of its isomer, furan (IE = 8.88 eV).[32,34] Although vinylketene at m/z = 68 has been proposed as an initial decomposition product of furfural for decades, it cannot be detected using various experimental methods.[15,18−20] Figure 3h exhibits the PIE spectrum of m/z = 96 ions. Only furfural can be distinguished by the onset at around 9.25 eV.[35] Vermeire et al. found that α-pyrone was a major product at low temperature, which was formed though furfural isomerization to formylvinylketene and a subsequent pericyclic ring closure reaction.[20] However, α-

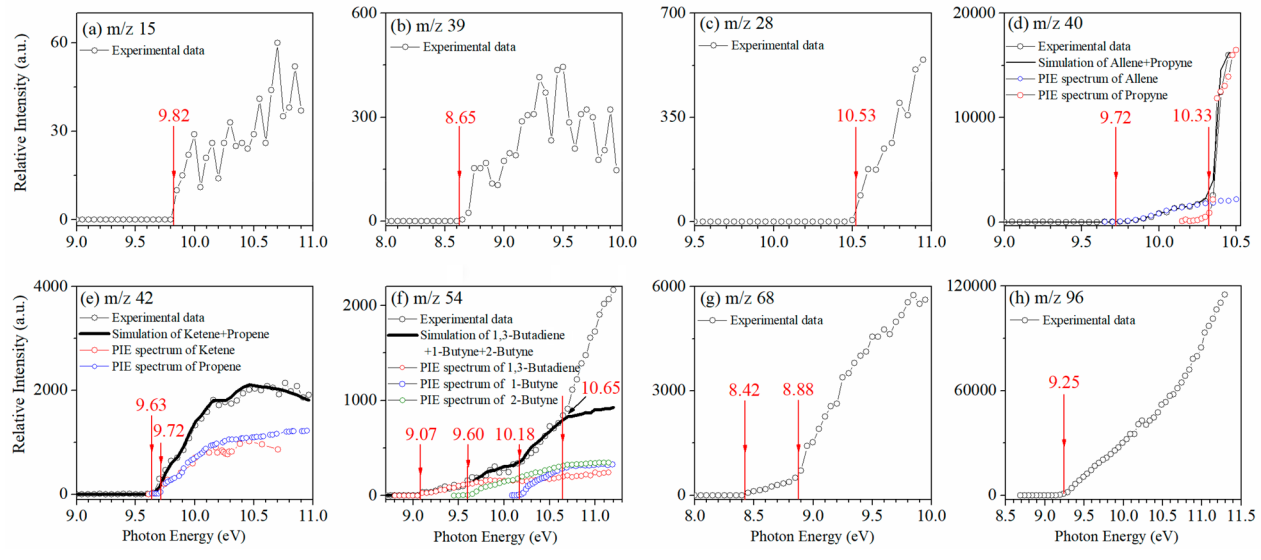

Figure 3. PIE spectra of m/z = 15, 39, 28, 40, 42, 54, 68, and 96 at 1273 K and 30 Torr.

DOI: 10.1021/acs.jpca.8b06261
J. Phys. Chem. A 2019, 123, 103−110

pyrone could not be identified because the PIE spectrum of m/z = 96 ions was similar to the PIE spectrum of furfural in the literature (see Figure S1 in the Supporting Information).[35] In addition to the species mentioned above, some other products, such as formaldehyde and aromatics, were also observed, and their experimental and literature IEs from the database of NIST are tabulated in Table 1. Methane (m/z = 16) and acetylene (m/z = 26) with higher IEs were identified at photon energies higher than 11 eV (see Figure S2).

Table 1. Assignment of the Product Species of Furfural Pyrolysis

			IE (eV)	
m/z	formula	species	literature	this work
15	CH_3	methyl radical	9.84	9.82
16	CH_4	methane	12.61	
26	C_2H_2	acetylene	11.40	
28	C_2H_4	ethylene	10.51	10.53
30	CH_2O	formaldehyde	10.88	10.88
39	C_3H_3	propargyl radical	8.67	8.65
40	C_3H_4	propyne	10.35	10.33
		allene	9.69	9.72
42	C_2H_2O	ketene	9.62	9.63
	C_3H_6	propene	9.73	9.72
52	C_4H_4	1-buten-3-yne	9.58	9.60
54	C_4H_6	1,3-butadiene	9.07	9.07
		1-butyne	10.18	10.18
		2-butyne	9.58	9.60
	C_3H_2O	2-propynal	10.62	10.65
68	C_4H_4O	furan	8.88	8.88
		vinylketene	8.40	8.42
78	C_6H_6	fulvene	8.36	8.40
		benzene	9.24	9.25
96	$C_5H_4O_2$	furfural	9.22	9.25

Unimolecular decomposition reactions, hydrogen atom abstraction, and hydrogen atom addition reactions coexist and play considerable roles in the decomposed process of most fuels.[11,14,21−23,36−39] With regard to furfural pyrolysis, only unimolecular decomposition reactions were discussed in previous lectures.[15,19,20] These major unimolecular decomposition reactions are summarized in Scheme 1. Hydrogen atom abstraction and addition reactions can be used to describe a comprehensive mechanistic picture of furfural pyrolysis. Moreover, hydrogen atom abstraction and addition reactions are very momentous during furfural pyrolysis. The significance and theoretical calculations of hydrogen atom abstraction and hydrogen atom addition reactions are discussed in detail below.

Scheme 1. Unimolecular Decomposition Pathways of Furfural

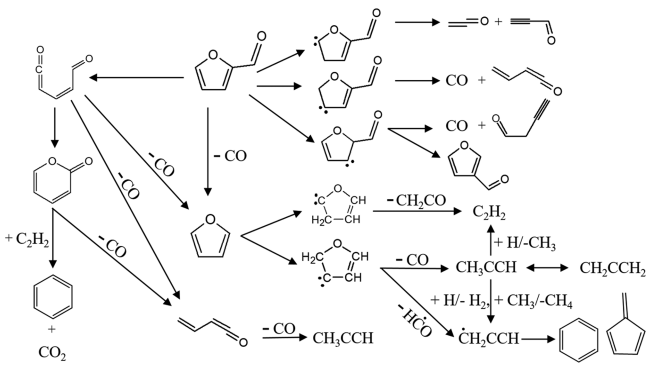

Unimolecular Decomposition Reactions of Furfural. Vermeire et al. investigated the unimolecular dissociation channels of furfural pyrolysis through theoretical calculations.[20] Some of the unimolecular dissociation channels are included in Scheme 1. Furfural undergoes isomerization reaction to form formylvinylketene (O═C═CH−CH═CH−CH═O). Furan and CO can be yielded from the dissociation of formylvinylketene. Formylvinylketene can convert into α-pyrone via a pericyclic ring closure reaction. Both α-pyrone and formylvinylketene can directly decompose to vinylketene and CO. α-Pyrone can also undergo a Diels−Alder reaction to form an adduct by combing with acetylene. The formed adduct subsequently dissociates to benzene and CO_2 via a reverse Diels−Alder reaction. Furfural can directly convert into furan and CO through a 1,2-hydrogen atom shift, which might be unimportant on account of a high energy barrier of 88.87 kcal/mol. Furthermore, 1,2-hydrogen atom shift reactions of furfural can also occur to yield three carbene species, including furfural-3-carbene, furfural-4-carbene, and furfural-5-carbene. Moreover, these three carbene species act as intermediates to further decompose. Furfural-3-carbene not only dissociates into 3-furaldehyde but also dissociates into 1-butynal and CO. Furfural-4-carbene and furfural-5-carbene can break into vinylketene + CO and ketene + 2-propynal (CH≡C−CH═O), respectively. Species such as furan, vinylketene, ketene, 2-propynal, and benzene were identified in our experiments.

Hydrogen Atom Addition and Hydrogen Atom Abstraction Pathways. In addition to unimolecular decomposition pathways, hydrogen atom abstraction reactions are very momentous to the pyrolysis of most hydrogen fuels and oxygenated fuels from previous lectures.[14,21−23,36−39] For example, hydrogen atom abstraction reactions contributed 50% at 30 Torr and 57% at 760 Torr to the consumption of 2,5-dimethylfuran based on ROP (rate of production) analysis.[39] Hydrogen atom addition reactions also play important roles during the decomposition processes of the fuels with a C═C bond, such as benzaldehyde.[15] Vasiliou et al. reported that benzaldehyde dissociated into a phenyl radical, hydrogen atom, and CO: C_6H_5CHO (+ M) → C_6H_5CO + H → C_6H_5 + CO + H[15]. Then the produced hydrogen atom can add to the phenyl ring of benzaldehyde to yield benzene (C_6H_6) and CO: C_6H_5CHO + H → C_6H_6CHO → C_6H_6 + CO + H[15]. From the above descriptions of benzaldehyde, hydrogen atom propagated the chain reaction and played a key role during the pyrolysis process of benzaldehyde.[15] Therefore, hydrogen atom addition reactions should be crucial to furfural pyrolysis due to the existence of a C═C bond in the furan ring of furfural.

Here, to further identify probable reaction pathways of furfural pyrolysis, hydrogen atom abstraction and hydrogen atom addition reactions were studied by theoretical calculations. These reaction pathways and corresponding potential energy surfaces related to furfural decomposition have been constructed by the CBS-QB3 method in Figures 4 and 5. The total energy of furfural and a hydrogen atom is defined as zero. Detailed geometry information of transition states involved in the thermal decomposition pathways is listed in the Supporting Information.

Figure 4 shows the potential energy surface of furfural through hydrogen atom addition reactions. The dissociation

DOI: 10.1021/acs.jpca.8b06261
J. Phys. Chem. A 2019, 123, 103−110

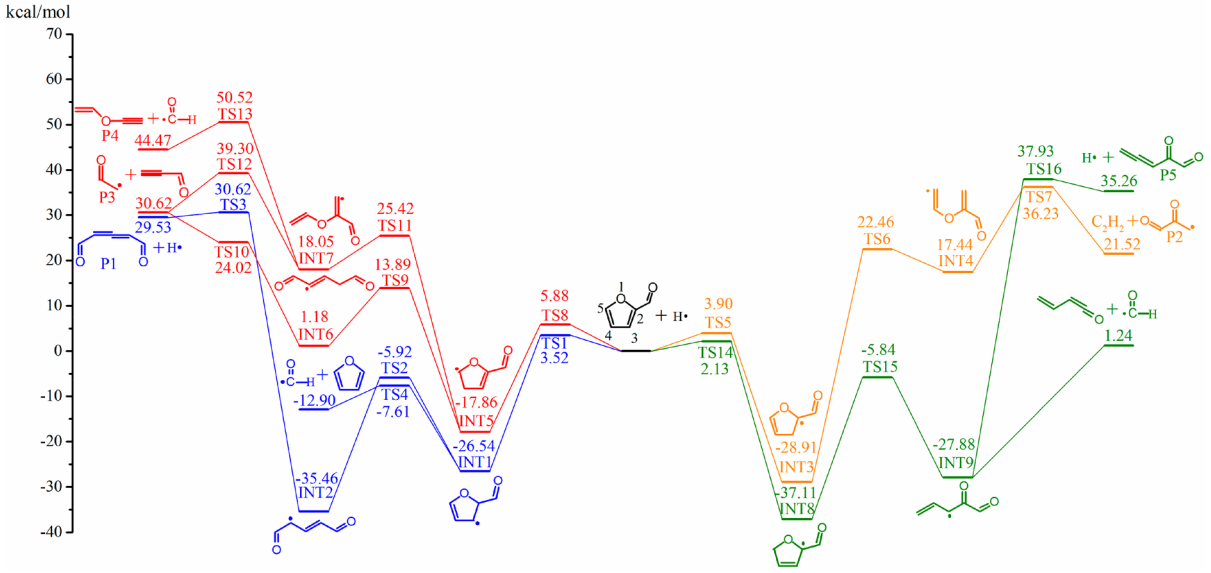

Figure 4. Potential energy surface of furfural through hydrogen atom addition reactions. Values are $\Delta_f H$ (0 K) calculated at the CBS//M06-2X/cc-pVTZ level of theory in kcal/mol.

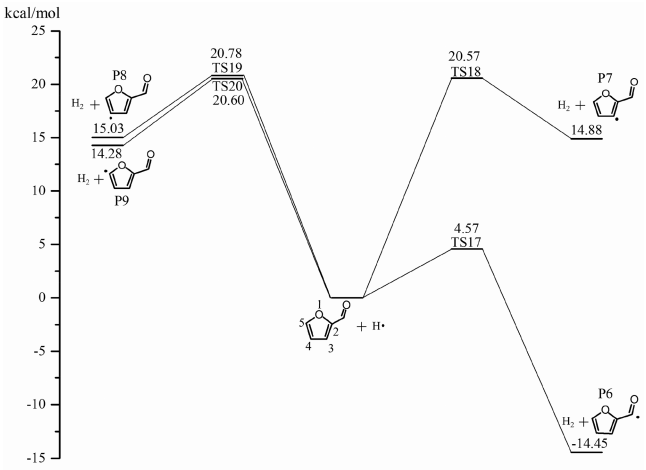

Figure 5. Potential energy surface of furfural through hydrogen atom abstraction reactions. Values are $\Delta_f H$ (0 K) calculated at the CBS//M06-2X/cc-pVTZ level of theory in kcal/mol.

reactions in Figure 4 can be categorized into four groups based on the type of products, containing the formation of a hydrogen atom, formyl radical, acetylene, and 2-propynal. Moreover, furan and vinylketene formed along with the releases of formyl radical can further decompose during furfural pyrolysis.

As presented in Figure 4, there are two channels to produce a hydrogen atom in the cases of hydrogen atom addition to furfural. (1) The addition of a hydrogen atom to C2 leads to produce an intermediate INT1 through a transition state 1 (TS1) surmounting an energy barrier of 3.52 kcal/mol. INT1 undergos cleavage of C2−O to form INT2 via TS2 with an activation energy of 20.62 kcal/mol. Subsequently, β-C−H bond dissociation of INT2 can occur to produce P1 + H via TS3 crossing an activation energy of 66.08 kcal/mol. P1 as one of the isomers of furfural was not detected in our experiments. (2) INT8 can be produced from hydrogen atom addition to C5 of furfural through TS14 over an energy barrier of 2.13 kcal/mol, followed by C5−O bond cleavage of INT8 to yield INT9 via TS15 with an energy barrier of 31.27 kcal/mol. INT9 can undergo dissociation of the β-C−H bond to produce P5 (keto,3,4-pentadienal) and a hydrogen atom via TS16 over a barrier of 65.81 kcal/mol. P5 as an isomer of furfural was not detected in our experiments.

There are three pathways to form HCO in Figure 4. (1) INT1, an intermediate from TS1, can also decompose to furan and HCO via TS4 with an energy barrier of 18.93 kcal/mol. The energy barrier for the formation of furan through this hydrogen atom addition reaction is much lower than the reported barrier for direct conversion of furfural to furan and CO through a 1,2-hydrogen atom shift (88.87 kcal/mol).[20] (2) INT5 as an adduct of hydrogen atom addition to C4 of furfural is formed through TS8 with an energy barrier of 5.88 kcal/mol, followed by cleavage of C3−C4 to produce a ring-opening intermediate INT7 via TS11 with an energy barrier of 43.28 kcal/mol. INT7 undergoes breakage of the β-C−C bond to produce HCO and P4 (1-ethenyloxyethyne) via TS13 with an activation energy of 32.47 kcal/mol. (3) INT9 formed from hydrogen atom addition to C5 of furfural can dissociate into HCO and vinylketene via β-C−C bond scission. Although there are several pathways to form vinylketene from unimolecular decomposition reported by Vermeire et al.,[20] the energy barrier for vinylketene formation of this hydrogen atom addition pathway is much lower than any one of the unimolecular decomposition pathways in the formation of vinylketene. HCO was not observed in our experiments because it will break into CO and H at high temperature.

Two pathways are considered for the formation of 2-propynal in Figure 4, both of which resulted from hydrogen atom addition to C4 of furfural. (1) Hydrogen atom addition to C4 of furfural will form INT5 through TS8. Furthermore, C2−O bond cleavage of INT5 results in the formation of INT6 through TS9 overcoming a barrier of 31.75 kcal/mol, followed by breakage of the β-C−C bond of INT6 to produce P3 and 2-propynal via TS10 with an energy barrier of 22.84 kcal/mol. (2) Intermediate INT5 can also undergo C3−C4 bond dissociation to produce INT7. Then β-C−O bond cleavage of INT7 leads to the generation of 2-propynal + P3 through TS12; the energy barrier of this reaction is 21.25 kcal/

DOI: 10.1021/acs.jpca.8b06261
J. Phys. Chem. A 2019, 123, 103−110

mol. As an active species, 2-propynal was identified in this work.

Only one pathway for C_2H_2 formation is established. As shown in Figure 4, a hydrogen atom adds to C3 of furfural to form an intermediate INT3 through TS5 with an activation energy of 3.90 kcal/mol. INT3 can further pyrolyze through C3−C4 bond cleavage or C5−O bond breakage. However, the transition state for C5−O bond cleavage of INT3 was not obtained in our theoretical calculations. INT3 undergoes C3−C4 bond cleavage to form INT4 through TS6 with an energy barrier of 51.37 kcal/mol. The β-C−O bond breakage of INT4 results in the formation of C_2H_2 and P2 via TS7 crossing an energy barrier of 18.79 kcal/mol.

By comparing the experimental results with theoretical calculations, we found that only several products, such as 2-propynal, furan, and vinylketene obtained in the theoretical calculations, can be identified in our experiments. Other pyrolysis products listed in Table 1 mainly come from further decomposition of furan and vinylketene because furfural and furan start to decompose at very close temperature (1090−1100 K).[7,9,19] The predominant decomposition pathways of furan are shown in Scheme 1. A detailed description of furan and vinylketene pyrolysis can be found in the Supporting Information.

Figure 5 displays the relative energies of the primary pyrolysis products, transition states, and intermediates during hydrogen atom abstraction reactions of furfural. Furfural decomposes to H_2 and P6 ($C_5H_3O_2$) through hydrogen atom abstraction reactions by the hydrogen atom attacking at the aldehyde group. This reaction was calculated to be exothermic by −14.45 kcal/mol, with a very low energy barrier (TS17) of 4.57 kcal/mol. Vermeire et al. reported the direct formation of P6 and a hydrogen atom by C−H bond scission with an energy barrier of 90.18 kcal/mol, which is much higher than the value through hydrogen atom abstraction. Isomeric $C_5H_3O_2$ and H_2 can also be formed via hydrogen atom abstraction from C3, C4, and C5 of furfural with endothermicity of 14.88, 15.03, and 14.28 kcal/mol, respectively. Corresponding energy barriers for these reactions are computed to be 20.57, 20.78, and 20.60 kcal/mol.

Aforementioned pathways for hydrogen atom addition and hydrogen atom abstraction reactions of furfural are summarized in Scheme 2. Besides, further β-scission reactions of P6, P7, P8, and P9 were inferred to improve the hydrogen atom abstraction mechanism. As shown in Scheme 2, radicals P6, P7, P8, and P9 are formed from hydrogen abstraction reactions. R5-1 is a channel to form O═C═CH−C≡C−CH═O + H through β-C−H dissociation of a ring-opening intermediate resulting from C2−O dissociation of P7. P8 can undergo disruption of the C5−O bond; then the following cleavage of β-C−C leads to the formation of HC═O + CH≡C−CH═C═O (R6-1). The furan ring of P6 can be opened by cracking the C2−O bond; then the ring-opening intermediate breaks into O═C═CH−CH═C═C═O + H through β-C−H dissociation (R8-1). The dissociation of C2−O opens the furan ring of P9 (R7-1), followed by β-C−H scission to form the same products as P6. Apart from R7-1, three other channels (R7-2, R7-3, and R7-4) can be formed from breaking of P9. R7-2 reveals that a ring-opening intermediate from C2−O bond fission of P9 further dissociates into CH≡C−CH═O (2-propynal) and CH═C═O by β-C−C scission. The ring-opening intermediate from C3−C4 breakage of P9 produces HC═O + CH≡C−O−C≡CH (R7-3) and CH≡C−CH═O + CH≡C−O (R7-4) through cleavage of β-C−C and β-C−O, respectively. The products CH═C═O from R7-2 and CH≡C−O R7-4 are isomers. In consideration of the products formed from the hydrogen atom abstraction reactions, only 2-propynal was detected in our experiments, indicating that the subsequent reactions of $C_5H_3O_2$ might have minor contributions in the consumption of furfural.

Scheme 2. Hydrogen Atom Addition and Hydrogen Atom Abstraction Reactions of Furfural

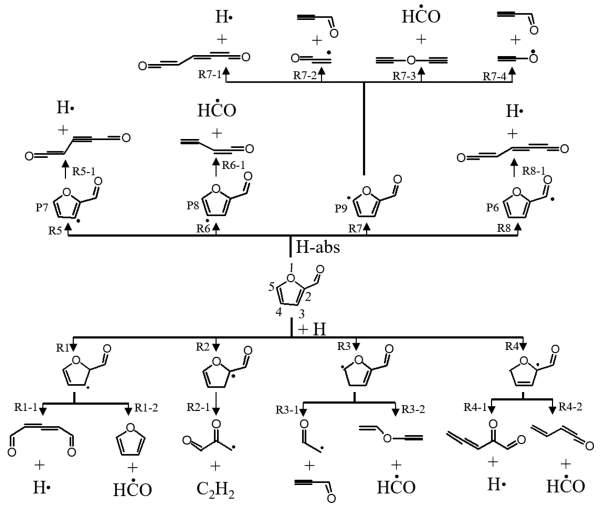

CONCLUSIONS

Experimental and theoretical studies were performed to investigate the thermal decomposition of furfural. The experimental study was conducted in a flow tube reactor at 30 Torr. The product species of furfural were monitored with SVUV-PIMS. The product species vinylketene and 2-propynal were directly observed in the thermal decomposition of furfural for the first time. The hydrogen atom addition and hydrogen atom abstraction reactions were calculated at the CBS-QB3 level. The primarily decomposed products of hydrogen atom addition and hydrogen atom abstraction reactions include the elimination of CO and the formation of acetylene, 2-propynal, furan, vinylketene, etc. Among them, the energy barrier of vinylketene formation is the lowest-energy pathway. Theoretical calculations shed further light on the thermal decomposition pathways.

ASSOCIATED CONTENT

Supporting Information

The Supporting Information is available free of charge on the ACS Publications website at DOI: 10.1021/acs.jpca.8b06261.

Mass spectra at various photon energies, comparison between the PIE spectrum of m/z 96 and the PIE spectrum of furfural, molecular geometry of the transition state (PDF)

AUTHOR INFORMATION

Corresponding Authors

*E-mail: panyang@ustc.edu.cn. (Y.P.).
*E-mail: zld@ustc.edu.cn. (L.Z.).
*E-mail: zjcheng@tju.edu.cn. (Z.C.).

ORCID

Lidong Zhang: 0000-0002-4924-1927

DOI: 10.1021/acs.jpca.8b06261
J. Phys. Chem. A 2019, 123, 103−110

Yang Pan: 0000-0002-9360-3809

Notes

The authors declare no competing financial interest.

■ ACKNOWLEDGMENTS

This work was supported by grants from the National Key Research and Development Program of China (2017YFA0402800), the Natural Science Foundation of China (No. 91545120), the Chinese Universities Scientific Fund, the Major/Innovative Program of Development Foundation of Hefei Center for Physical Science and Technology (2016FXCX008), and the Key Program of Research and Development of Hefei Science Center CAS (2018HSC-KPRD002), and the Users with Excellence Project of Hefei Science Center CAS (2018HSC-UE001).

■ REFERENCES

(1) Wang, S.; Dai, G.; Yang, H.; Luo, Z. Lignocellulosic Biomass Pyrolysis Mechanism: A State-of-the-Art Review. *Prog. Energy Combust. Sci.* **2017**, *62*, 33−86.
(2) Bridgwater, A. V. Review of Fast Pyrolysis of Biomass and Product Upgrading. *Biomass Bioenergy* **2012**, *38*, 68−94.
(3) Czernik, S.; Bridgwater, A. V. Overview of Applications of Biomass Fast Pyrolysis Oil. *Energy Fuels* **2004**, *18*, 590−598.
(4) Lange, J. P.; van der Heide, E.; van Buijtenen, J.; Price, R. Furfural—A Promising Platform for Lignocellulosic Biofuels. *ChemSusChem* **2012**, *5*, 150−166.
(5) Urness, K. N. *A Molecular Picture of Biofuel Decomposition: Pyrolysis of Furan and Select Furanics*; University of Colorado at Boulder, 2014.
(6) Winfough, M.; Voronova, K.; Muller, G.; et al. Furfural: The Unimolecular Dissociative Photoionization Mechanism of the Simplest Furanic Aldehyde. *J. Phys. Chem. A* **2017**, *121*, 3401−3410.
(7) Grela, M. A.; Amorebieta, V. T.; Colussi, A. J. Very Low Pressure Pyrolysis of Furan, 2-Methylfuran and 2, 5-Dimethylfuran. The Stability of the Furan Ring. *J. Phys. Chem.* **1985**, *89*, 38−41.
(8) Zhou, X.; Li, W.; Mabon, R.; Broadbelt, J. L. A Critical Review on Hemicellulose Pyrolysis. *Energy Technol.* **2017**, *5*, 52−79.
(9) Cheng, Z.; Tan, Y.; Wei, L.; et al. Experimental and Kinetic Modeling Studies of Furan Pyrolysis: Fuel Decomposition and Aromatic Ring Formation. *Fuel* **2017**, *206*, 239−247.
(10) Urness, K. N.; Guan, Q.; Golan, A.; et al. Pyrolysis of Furan in a Microreactor. *J. Chem. Phys.* **2013**, *139*, 124305.
(11) Cheng, Z.; Niu, Q.; Wang, Z.; et al. Experimental and Kinetic Modeling Studies of Low-Pressure Premixed Laminar 2-Methylfuran Flames. *Proc. Combust. Inst.* **2017**, *36*, 1295−1302.
(12) Somers, K. P.; Simmie, J. M.; Metcalfe, W. K.; Curran, H. J. The Pyrolysis of 2-Methylfuran: A Quantum Chemical, Statistical Rate Theory and Kinetic Modelling Study. *Phys. Chem. Chem. Phys.* **2014**, *16*, 5349−5367.
(13) Sendt, K.; Bacskay, G. B.; Mackie, J. C. Pyrolysis of Furan: Ab Initio Quantum Chemical and Kinetic Modeling Studies. *J. Phys. Chem. A* **2000**, *104*, 1861−1875.
(14) Cheng, Z.; He, S.; Xing, L.; et al. Experimental and Kinetic Modeling Study of 2-Methylfuran Pyrolysis at Low and Atmospheric Pressures. *Energy Fuels* **2017**, *31*, 896−903.
(15) Vasiliou, A. K.; Kim, J. H.; Ormond, T. K.; Piech, K. M.; et al. Biomass Pyrolysis: Thermal Decomposition Mechanisms of Furfural and Benzaldehyde. *J. Chem. Phys.* **2013**, *139*, 104310.
(16) Patwardhan, P. R.; Brown, R. C.; Shanks, B. H. Product Distribution from the Fast Pyrolysis of Hemicellulose. *ChemSusChem* **2011**, *4*, 636−643.
(17) Li, Z.; Liu, C.; Xu, X.; et al. A Theoretical Study on the Mechanism of Xylobiose during Pyrolysis Process. *Comput. Theor. Chem.* **2017**, *1117*, 130−140.
(18) Hurd, C. D.; Goldsby, A. R.; Osborne, E. N. Furan Reactions. II. Furan from Furfural. *J. Am. Chem. Soc.* **1932**, *54*, 2532−2536.
(19) Grela, M. A.; Colussi, A. J. Kinetics and Mechanism of the Thermal Decomposition of Unsaturated Aldehydes: Benzaldehyde, 2-Butenal, and 2-Furaldehyde. *J. Phys. Chem.* **1986**, *90*, 434−437.
(20) Vermeire, F. H.; Carstensen, H. H.; Herbinet, O.; et al. The Thermal Decomposition of Furfural: Molecular Chemistry Unraveled. *Proc. Combust. Inst.* **2018**, DOI: 10.1016/j.proci.2018.05.119.
(21) Zhang, Y.; Cao, C.; Li, Y.; Yuan, W.; et al. Pyrolysis of n-Butylbenzene at Various Pressures: Influence of Long Side-Chain Structure on Alkylbenzene Pyrolysis. *Energy Fuels* **2017**, *31*, 14270−14279.
(22) Cai, J.; Zhang, L.; Zhang, F.; et al. Experimental and Kinetic Modeling Study of n-Butanol Pyrolysis and Combustion. *Energy Fuels* **2012**, *26*, 5550−5568.
(23) Zhai, Y.; Feng, B.; Yuan, W.; et al. Experimental and Modeling Studies of Small Typical Methyl Esters Pyrolysis: Methyl Butanoate and Methyl Crotonate. *Combust. Flame* **2018**, *191*, 160−174.
(24) Zhou, Z.; Wang, Y.; Tang, X.; et al. A New Apparatus for Study of Pressure-dependent Laminar Premixed Flames with Vacuum Ultraviolet Photoionization Mass Spectrometry. *Rev. Sci. Instrum.* **2013**, *84*, No. e014101.
(25) Wang, Y.; Yang, J.; Pan, Y.; Ma, H.; Li, Y.; Qi, F. On-Line Photoionization Mass Spectrometric Study On the Behavior of Ammonia Poisoning on HUSY for the Catalytic Pyrolysis of Polypropylene. *Chin. J. Chem. Phys.* **2016**, *29*, 681−686.
(26) Zhu, Y.; Chen, X.; Wang, Y.; Wen, W.; Wang, Y.; Yang, J.; Zhou, Z.; Zhang, L.; Pan, Y.; Qi, F. Online Study on the Catalytic Pyrolysis of Bituminous Coal over the HUSY and HZSM-5 with Photoionization Time-of-Flight Mass Spectrometry. *Energy Fuels* **2016**, *30*, 1598−1604.
(27) Wang, Y.; Wang, Y.; Zhu, Y.; Pan, Y.; Yang, J.; Li, Y.; Qi, F. Influence of Thermal Treatment of HUSY on Catalytic Pyrolysis of Polypropylene: An Online Photoionization Mass Spectrometric Study. *Energy Fuels* **2016**, *30*, 5122−5129.
(28) Frisch, M. J.; Trucks, G. W.; Schlegel, H. B.; Scuseria, G. E.; Robb, M. A.; Cheeseman, J. R.; Zakrzewski, V. G.; Montgomery, J. A., Jr.; Stratmann, R. E.; Burant, J. C.; Dapprich, S.; Millam, J. M.; Daniels, A. D.; Kudin, K. N.; Strain, M. C.; Farkas, O.; Tomasi, J.; Barone, V.; Cossi, M.; Cammi, R.; Munnucci, B.; Pomelli, C.; Adamo, C.; Clifford, S.; Ochterski, J.; Petersson, G. A.; Ayala, P. Y.; Cui, Q.; Morokuma, K.; Rega, N.; Salvador, P.; Dannenberg, J. J.; Malick, D. K.; Rabuck, A. D.; Raghavachari, K.; Foresman, J. B.; Cioslowski, J.; Ortiz, J. V.; Baboul, A. G.; Stefanov, B. B.; Liu, G.; Liashenko, A.; Pikorz, P.; Komaromi, I.; Gomperts, R.; Martin, R. L.; Fox, D. J.; Keith, T.; Al-Laham, M. A.; Peng, C. Y.; Nakayakkara, A.; Challacombe, M.; Gill, P. M. W.; Johnson, B.; Chen, W.; Wong, M. W.; Andres, J. L.; Gonzalez, C.; Challacombe, M.; Gill, P. M.W.; Johnson, B.; Chen, W.; Wong, M. W.; Andres, J. L.; Gonzales, C.; Head-Gordon, M.; Replogle, E. S.; Pople, J. A. *Gaussian 03*, revision C, 2nd ed.; Gaussian, Inc.: Pittsburgh, PA, 2004.
(29) Taatjes, C. A.; Osborn, D. L.; Selby, T. M.; Meloni, G.; et al. Absolute Photoionization Cross-Section of the Methyl Radical. *J. Phys. Chem. A* **2008**, *112*, 9336−9343.
(30) Robinson, J. C.; Sveum, N. E.; Neumark, D. M. Determination of Absolute Photoionization Cross Sections for Vinyl and Propargyl Radicals. *J. Chem. Phys.* **2003**, *119*, 5311−5314.
(31) Cool, T. A.; Wang, J.; Nakajima, K.; Taatjes, T. A. Photoionization Cross Sections for Reaction Intermediates in Hydrocarbon Combustion. *Int. J. Mass Spectrom.* **2005**, *247*, 18−27.
(32) Yang, B.; Wang, J.; Cool, T. A.; Hansen, N. Absolute Photoionization Cross-Sections of Some Combustion Intermediates. *Int. J. Mass Spectrom.* **2012**, *309*, 118−128.
(33) Opitz, J. Photoionization of Propynal in the Gas Phase. *Int. J. Mass Spectrom. Ion Processes* **1991**, *107*, 503−513.
(34) Holmes, J. L.; Terlouw, J. K. Structures of $[C_4H_4O]^+$ Ions Produced from 2-and 4-Pyrone. *J. Am. Chem. Soc.* **1979**, *101*, 4973−4975.
(35) Smith, A. R.; Meloni, G. Absolute Photoionization Cross Sections of Furanic Fuels: 2-Ethylfuran, 2-Acetylfuran and Furfural. *J. Mass Spectrom.* **2015**, *50*, 1206−1213.

DOI: 10.1021/acs.jpca.8b06261
J. Phys. Chem. A 2019, 123, 103−110

(36) Zhai, Y.; Ao, C.; Feng, B. Experimental and Kinetic Modeling Investigation on Methyl Decanoate Pyrolysis at Low and Atmospheric Pressures. *Fuel* **2018**, *232*, 333−340.
(37) Zhang, T.; Zhang, L.; Hong, X.; et al. An Experimental and Theoretical Study of Toluene Pyrolysis with Tunable Synchrotron VUV Photoionization and Molecular-beam Mass Spectrometry. *Combust. Flame* **2009**, *156*, 2071−2083.
(38) Liu, C.; Ye, L.; Yuan, W.; et al. Investigation on Pyrolysis Mechanism of Guaiacol as Lignin Model Compound at Atmospheric Pressure. *Fuel* **2018**, *232*, 632−638.
(39) Cheng, Z.; Xing, L.; Zeng, M.; et al. Experimental and Kinetic Modeling Study of 2, 5-Dimethylfuran Pyrolysis at Various Pressures. *Combust. Flame* **2014**, *161*, 2496−2511.
(40) Pines, H.; Haag, W. O. Alumina: Catalyst and Support I. Alumina, Its Intrinsic Acidity and Catalytic Activity. *J. Am. Chem. Soc.* **1960**, *82*, 2471−2483.
(41) Cheng, Z. J.; Xing, L L.; Zeng, M. R. Experimental and Kinetic Modeling Study of 2,5-Dimethylfuran Pyrolysis at Various Pressures. *Combust. Flame* **2014**, *161*, 2496−2511.

DOI: 10.1021/acs.jpca.8b06261
J. Phys. Chem. A 2019, 123, 103−110